ELSEVIER

Journal of Power Sources 85 (2000) 269–278

JOURNAL OF POWER SOURCES

www.elsevier.com/locate/jpowsour

Thermal and electrochemical studies of carbons for Li-ion batteries 2. Correlation of active sites and irreversible capacity loss

T. Tran [a], B. Yebka [b], X. Song [c], G. Nazri [b], K. Kinoshita [c,*], D. Curtis [b]

[a] *Chemistry and Materials Science Department, Lawrence Livermore National Laboratory, Livermore, CA 94550, USA*
[b] *Department of Chemistry, University of Michigan, Ann Arbor, MI 48109, USA*
[c] *Environmental Energy Technologies Division, Lawrence Berkeley National Laboratory, Berkeley, CA 94720, USA*

Received 17 March 1999; accepted 6 July 1999

Abstract

Thermal gravimetric analysis (TGA) and differential thermal analysis (DTA) involving air oxidation of fluid coke, coal-tar pitch delayed coke and needle coke suggested that active sites are present which can be correlated to the crystallographic parameters, L_a and L_c, and the $d(002)$ spacing. This finding was extended to determine the relationship between active sites on carbon and their role in catalyzing electrolyte decomposition leading to irreversible capacity loss (ICL) in Li-ion batteries. Electrochemical data from this study with graphitizable carbons and from published literature were analyzed to determine the relationship between the physical properties of carbon and the ICL during the first charge/discharge cycle. Based on this analysis, we conclude that the active surface area, and not the total BET surface area, has an influence on the ICL of carbons for Li-ion batteries. This conclusion suggests that the carbon surface structure plays a significant role in catalyzing electrolyte decomposition.

Keywords: Irreversible capacity; Carbon structure; Li-ion batteries

1. Introduction

Nonaqueous electrolytes react on the surface of carbon electrodes for Li-ion batteries during the initial charge/discharge cycles. The decomposition reactions result in the irreversible consumption of Li ions and the formation of the so-called SEI (solid electrolyte interface) layer. The formation of the SEI layer is associated with electrochemical reactions that contribute to the irreversible capacity loss (ICL). Numerous studies [1–9] have reported a relationship between the ICL and surface area, i.e., higher ICL is obtained with carbons of higher surface area. The correlation between the surface area and ICL suggests that both the basal plane sites and edge sites on the carbon surface are effective sites for electrolyte decomposition. Barsoukov et al. [6] suggested that the electrochemically active area of carbon is the geometric surface area of the particle. In essence, this corresponds to the total surface area of the nonporous carbon particles. However, a study on single-crystal graphite by Tran and Kinoshita [10] clearly showed that the current density for intercalation/deintercalation of Li^+ ions on the basal planes was considerably lower than that on the edge planes, which agrees with the earlier study of Yamamoto et al. [11]. Unfortunately, the ICL was not readily discernible from the cyclic voltammograms. The conclusion from these studies is that the edge and basal plane sites have a large difference in reactivity for the intercalation/deintercalation reactions involving Li^+ ions. Bar-Tow et al. [12] observed by X-ray photoelectron spectroscopy that the SEI layer was thinner on the basal-plane surface of HOPG than that on the edge plane. The thin SEI layer on the basal plane is likely associated with electrochemical reactions on the edge or defect sites that are present on the inactive surface.

Winter et al. [5] presented an excellent summary of background information on the origin of the SEI layer and the ICL. It is evident that there are many factors contributing to the formation of the SEI layer on carbon, including the electrolyte composition, impurities, carbon structure and surface complexes. The latter two of these factors have some relationship to the active surface area. For example, a highly graphitic carbon is likely to have a crystal structure that contains a significant fraction of basal plane sites

* Corresponding author. Tel.: +1-510-486-7389; fax: +1-510-486-4260; E-mail: k_kinoshita@lbl.gov

0378-7753/00/$ - see front matter
PII: S0378-7753(99)00343-2

at the surface and a small fraction of surface complexes. On the other hand, amorphous carbons can have a significant fraction of surface edge sites and an appreciable amount of surface complexes, which are located at the edge sites. The net result is that the edge sites and surface complexes are expected to influence the ICL by acting as the active sites for electrolyte decomposition. The concept that certain sites (i.e., prismatic surface sites) contribute to the ICL was recognized by Winter et al. [5], and they further noted that the basal plane sites were relatively inactive. More recently, Chung et al. [7] reached a similar conclusion that the edge and basal plane sites on carbon showed different activities toward electrolyte decomposition. Finally, it should be noted that even as far back as the 1970s, several research groups [13,14] recognized the significance of catalysis on the reactivity of graphite surfaces for Li intercalation.

An interesting analysis was presented by Shiota et al. [15] that described the results of a correlation between the contact heat of wetting of benzene (Bz) and hexane (Hx) and the ICL on mesocarbon microbeads (MCMBs). An empirical parameter (X) was derived

$$X = \mathrm{Bz}/(\mathrm{Bz} + \mathrm{Hx}) \quad (1)$$

that exhibited a relationship to the ICL, i.e., ICL increased when $X \rightarrow 1$. Shiota further concluded that the heat of wetting was associated with the magnitude of the active surface area of the MCMBs. Thus, the ICL is a function of the active surface area.

The results obtained by thermal measurements indicate that the surface area and crystallographic structure play an important role in the oxidation rate and ignition temperature of carbonaceous materials in air [16–19]. The edge sites and defect sites are believed to be active sites for the oxidation reactions of carbon. Thermal analysis of the oxidation behavior of carbon blacks showed that the temperature at which 15% carbon weight loss is attained (T_{15}) decreased with an increase in the surface area of the carbon [16]. However, the active surface area and not the total surface area (TSA) is the important parameter controlling the oxidation rate of carbons [20]. TGA measurements [19] showed that the ignition temperature (T_i) of ball-milled graphite and active carbons decreased with more ball milling. These results indicate that the disordered carbons, which formed by ball milling, have more active sites that oxidized more rapidly. DTA studies [18] revealed that the maximum temperature (T_m) in the exotherm during air oxidation increased with an increase in the crystallite dimension perpendicular to the graphite layer planes, L_c, and a decrease in the $d(002)$ spacing. The studies by Radovic et al. [20] suggested that the magnitude of the crystallite dimension parallel to the graphite layer planes, L_a, is a good measure of the fraction of active sites associated with carbons. The relative fraction of active sites on carbon decreases as L_a increases.

The thermal oxidation studies of carbon [20] suggest that the edge sites are catalytically more active than the basal plane sites, which raises the question, ''Are the edge sites on carbon, active sites for electrolyte decomposition?'' The studies mentioned above [1–9] provide an insight into the relationship between surface area and ICL of graphite and other carbonaceous materials. In our studies, we would like to develop a more specific correlation between the ICL and the active surface area of various types of carbons, ranging from graphitic to amorphous materials.

Based on the observations described above, we decided to utilize thermal analysis to obtain information on the active sites on carbons, and to utilize these findings to develop a correlation with the ICL on the same carbons in nonaqueous electrolytes for Li-ion batteries. The results of a study on the thermal analysis of air oxidation of soft carbons (fluid coke, needle coke and coal-tar pitch coke) were presented in Part 1 [21]. The aim of this paper is to analyze the connection between the ICL and the relative amount of active sites on carbon.

2. Experimental details

Details on the properties and processing of the petroleum (fluid and needle coke) and coal-tar pitch cokes used in this study are described in Part 1 [21]. The cokes were obtained from Superior Graphite (Chicago, IL) and the as-received carbons are typical produced at a temperature of around 1400°C. The physicochemical properties of the coke were modified by heat treatment at temperatures up to 2800°C in an inert environment. Other artificial (CPC) and natural graphites (BG-34, BG-35, CN-39 and CN-39A) were also obtained from Superior Graphite for investigation.

The crystallographic structure of the carbonaceous materials were studied by conventional powder X-ray diffraction (XRD) using a Siemens 500 diffractometer with CuK_α radiation, 40-kV anodic voltage and 30-mA current. The average crystallite dimensions, L_a, in the graphite lattice plane (a-axis direction) and L_c, perpendicular to the graphite plane (c-axis direction), were estimated from the half widths of the (110) and (002) diffraction peaks, respectively. The following equations from the X-ray diffraction patterns were used to determine the crystallite dimensions:

$$L_c(002) = 0.89\lambda/(B_{002}\cos\theta_{002}) \quad (2)$$

$$L_a(110) = 1.84\lambda/(B_{110}\cos\theta_{110}) \quad (3)$$

where λ is the wavelength of CuK_α ($\lambda = 0.15418$ nm), B_{110} and B_{002} are the width at half-maximum of the (110) and (002) diffraction peaks, and θ_{110} and θ_{002} are the corresponding Bragg diffraction angles.

Two electrode fabrication and electrochemical procedures were used to measure the reversible capacity and ICL of the various carbonaceous materials. In brief, the electrodes containing coke powders (typically 90%) were prepared according to a procedure that uses pyrolyzed phenolic resin as the binder [22,23]. In experiments with other carbons, thin-film electrodes were prepared from slurries of carbon powder (85.8 wt.%), Shawinigan acetylene black (8.6 wt.%), and an elastomer binder (5.6 wt.%), ethylene propylene diene monomer (EPDM) in xylene. The mixture was micronized to form an ink-slurry that was applied to a copper-foil current collector with precise thickness control to obtain a highly uniform coating. After coating, the film electrodes were dried overnight at 100°C in a vacuum-oven antechamber of a dry box. The electrodes were hot pressed in a dry box (<1 ppm moisture, oxygen and nitrogen) to obtain good adhesion and a glassy smooth surface. The typical electrode loading was about 20 mg/cm^2 and the electrode thickness was close to 120 μm.

The electrochemical performance of the carbon electrodes was determined in various electrolytes. Solvents used were ethylene carbonate (EC, FLUKA), diethyl carbonate (DEC, FLUKA), dimethyl carbonate (DMC, FLUKA) and propylene carbonate (PC, FLUKA). Different combinations of electrolytes were prepared by adding 1 M lithium hexafluorophosphate ($LiPF_6$, Hashimoto) or 0.5 M trifluoromethane sulfonimide ($LiN(CF_3SO_2)_2$ (tradename HQ115, 3M) to mixtures of the carbonate solvents. The electrochemical experiments were conducted in a three-electrode cell with lithium foils as both counter and reference electrodes or two-electrode cells with a lithium foil counter electrode. Charge and discharge tests were typically done at $C/24$ rate.

3. Results and discussion

As mentioned above, several studies indicate that the ICL increases approximately linearly with an increase in the surface area of the carbon. This relationship suggests that the carbon surface has no clearly dominant specific sites which are catalytically active for electrolyte decomposition, or in other words, the fraction of active sites remains constant, independent of the surface area. A survey of recent publications and data generated in the present study were evaluated to better understand the relationship between the surface area and crystallite parameters of carbon and the ICL. Table 1 summarizes the source of the data used in the evaluation. It is apparent from the list in Table 1 that a variety of carbonaceous materials, ranging from highly graphitic carbons to highly disordered hard carbons, and different electrolytes were considered. In addition, different procedures were used to obtain the reversible and irreversible capacities.

3.1. Relationship between ICL and surface area

Fig. 1 shows a plot of the specific ICL activity (i.e., ICL/BET surface area) vs. the BET surface area for data obtained with graphitizable carbons in this study. These carbons consist of heat-treated petroleum (fluid and needle coke) and coal-tar pitch cokes, as well as artificial and natural graphites. Furthermore, two different electrolytes were used in the experiments. Despite the differences in the types of graphitizable carbons, electrolytes and experimental conditions, the plot in Fig. 1 shows that the specific ICL activity changes as a function of the surface area. The specific ICL activity decreases from >30 mA h/m^2 at

Table 1
Summary of carbon and electrolytes used in analysis

Carbon samples and/or precursors	Electrolyte	Reference
Petroleum and pitch cokes	1 M $LiN(SO_2CF_3)$/EC-DMC (1:1)	This study
Natural and artificial graphites	1 M $LiPF_6$/EC-DEC (1:2)	
Natural and artificial graphites	1 M $LiN(SO_2CF_3)$/EC-DMC (1:2)	Winter et al. [5]
Natural and artificial graphites, MCMB	1 M $LiPF_6$/EC-DEC	Chung et al. [7]
	1 M $LiPF_6$/EC-DEC-PC	
Carbonized organic polymers	1 M $LiPF_6$/EC-DEC (2:1)	Jung et al. [9]
Petroleum pitch, PVC, PVDF, PPS	1 M $LiPF_6$/EC-DEC (3:7)	Zheng et al. [24]
Epoxy novolac resin		
Carbonized sucrose	1 M $LiPF_6$/EC-DEC (1:2)	Buiel et al. [25]
CVD on carbonized sucrose	1 M $LiPF_6$/EC-DEC (1:2)	Buiel and Dahn [26]
Natural and artificial graphites, carbon black	1 M $LiPF_6$/EC	Fujimoto et al. [27]
Pitch and petroleum cokes	1 M $LiPF_6$/PC	
Natural graphite, pitch coke, MCMB	1 M $LiClO_4$ in various solvents	Iijima et al. [28]
Pitch and PAN carbon fibers		
Carbonized phenolic resins		
MCMB	1.5 M $LiPF_6$ in various solvents	Ohta et al. [29]
PAN-based hard carbon	1 M $LiPF_6$/EC-DMC (2:1)	Jung et al. [30]
Graphitized carbon fibers	1 M $LiClO_4$/EC-DEC (1:1)	Tatsumi et al. [31]
Carbonized phenolic resins	1 M $LiClO_4$/EC-DEC (3:7)	Xiang et al. [32]

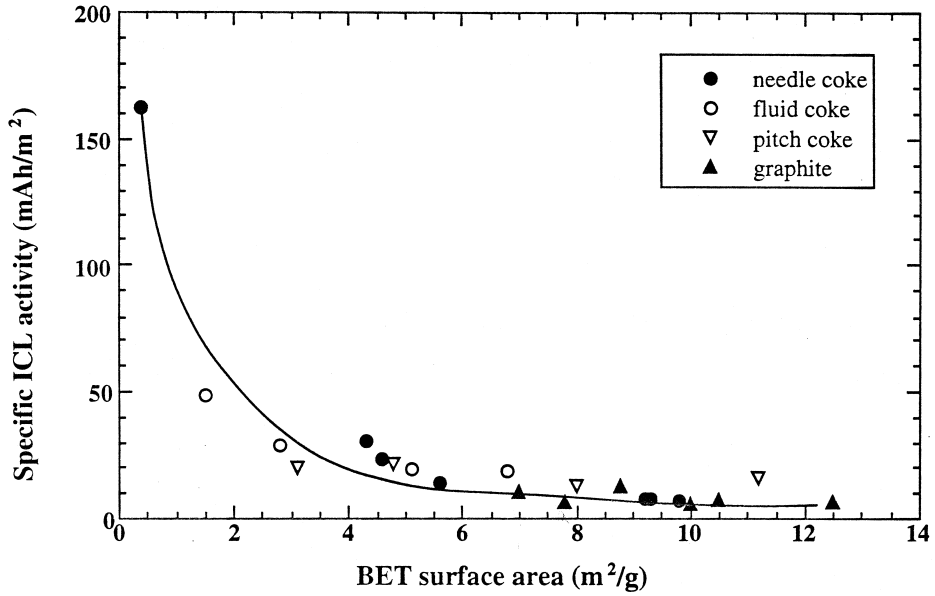

Fig. 1. Specific activity of various carbons for electrolyte decomposition plotted vs. BET surface area. Line indicates trend of the data.

low BET surface area (i.e., < 5 m^2/g) to around 10 mA h/m^2 at higher surface areas (e.g., > 10 m^2/g). The results suggest that the carbon surface is not uniformly active for electrolyte decomposition, otherwise the specific activity would be constant, independent of the surface area.

Published data on the ICL of carbons were analyzed to determine if our observations could be extended to other studies. A brief description of the different carbons and electrolytes, and the source of the data are summarized in Table 1. The composite results for the specific ICL activity and the BET surface area are presented in Fig. 2. Because of the broad range of specific activities and surface areas, a log–log plot is presented. The results in Fig. 2 show a linear trend in which the specific ICL activity decreases as the BET surface area increases, which is consistent with the data presented in Fig. 1. The range of the specific ICL activities and BET surface areas is surprisingly large, both varying by more than two orders-of-magnitude. The carbons with the highest surface area, which are hard carbons, have the lowest specific ICL activity. On the other hand, graphitizable or soft carbons that have a low fraction of active surface area after heat treatment exhibit the highest specific ICL activity. The trend of the specific ICL activi-

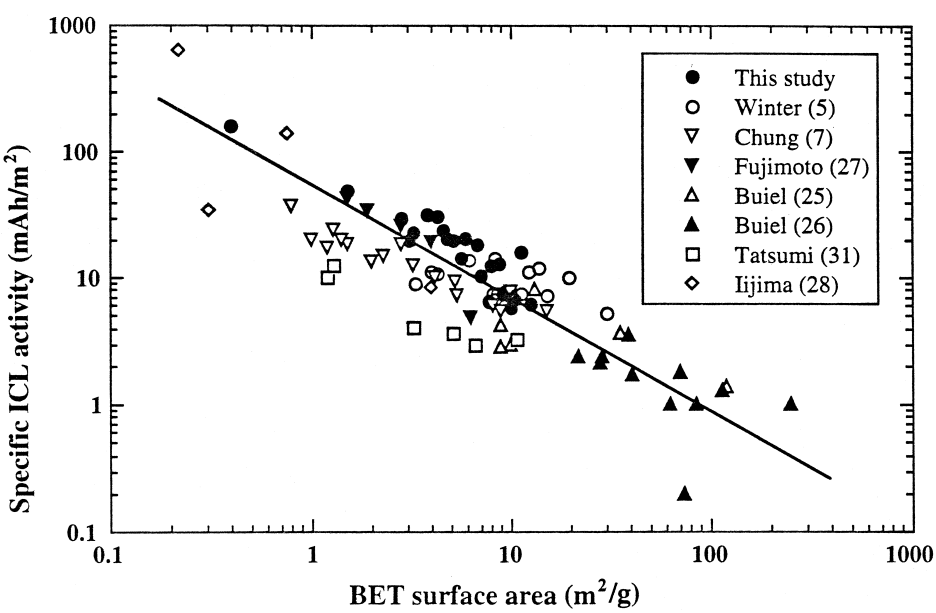

Fig. 2. Composite results for the specific activity of various carbons for electrolyte decomposition plotted vs. BET surface area. See Table 1 for source of the data. Line indicates trend of the data.

ties as a function of the total surface area is consistent with the earlier conclusions by Winter et al. [5], Chung et al. [7] and Shiota et al. [15], and from the data in Fig. 1. In the present paper, we extend the analysis by these research groups and others to illustrate the role of the carbon active sites on electrolyte decomposition and the ICL.

The electrolyte-wetted surface area is assumed to correspond to the measured BET surface area. The ratio of the wetted surface and the measured BET surface area is expected to be close to one for lower surface area, relatively nonporous carbons (< 5 m^2/g). Even though the fraction of the wetted surface is unknown and difficult to estimate for high-surface-area carbons, it is unlikely that this plays a significant role because of the continuously trend that is observed in the data. Therefore, we believe that the trends in the data that are presented here are not artifacts associated with variations in the relative fraction of the wetted surface area.

In Part 1 [21], experimental results were presented that showed an empirical correlation exists between the thermal parameters and the crystallographic parameters. From that analysis we further indicated that the fraction of active sites was an important factor influencing the ignition temperature (T_i), maximum temperature (T_m) and the temperature at 15% weight loss (T_{15}). If the ICL is related to the amount of active sites, then ICL should show a relationship to these thermal parameters. A plot of T_m vs. ICL is presented in Fig. 3 for the petroleum (fluid and needle coke) and coal-tar pitch cokes. The trend of the data suggests that ICL decreases as T_m increases. This relationship is consistent with the observation that ICL changes in concert with the concentration of active sites.

3.2. Dependence of ICL on crystallographic parameter L_a

Yamamoto et al. [11] conducted electrochemical experiments with graphite pellets that demonstrate the importance of edge sites as active sites for electrolyte decomposition in propylene carbonate. Natural graphite flakes were compressed at high pressure (40 MPa) to form a pellet with the upper and lower faces consisting of oriented basal planes and the circumference consisted of edge sites. Cyclic voltammetry demonstrated that no electrochemical reaction was evident on the basal plane surface, but was clearly present on the edge sites. These experiments demonstrate that the surface structure of the carbon is an important factor for electrolyte decomposition and the ICL.

Matsumura et al. [33] also noted the role of active sites in contributing to electrolyte decomposition. They concluded that active sites were present on the surface and in the bulk of the carbon particle, and furthermore, that functional groups such as –OH and carbon radicals are the active sites. On the other hand, Fujimoto et al. [27] concluded that functional groups have a minor influence on the ICL. Finally, it should be noted that Peled et al. [34] concluded that the SEI layer formed at the edge sites on graphite.

If specific sites, such as the edge sites, exist on the carbon surface, and which are responsible for electrolyte decomposition, then there should be a relationship between the fraction of edge sites and the ICL for the various carbons. In the present study, a model is proposed to show a correlation between the active surface area and the ICL. Radovic et al. [20] suggested a connection between the crystallite diameter, L_a, and the active surface area; i.e.,

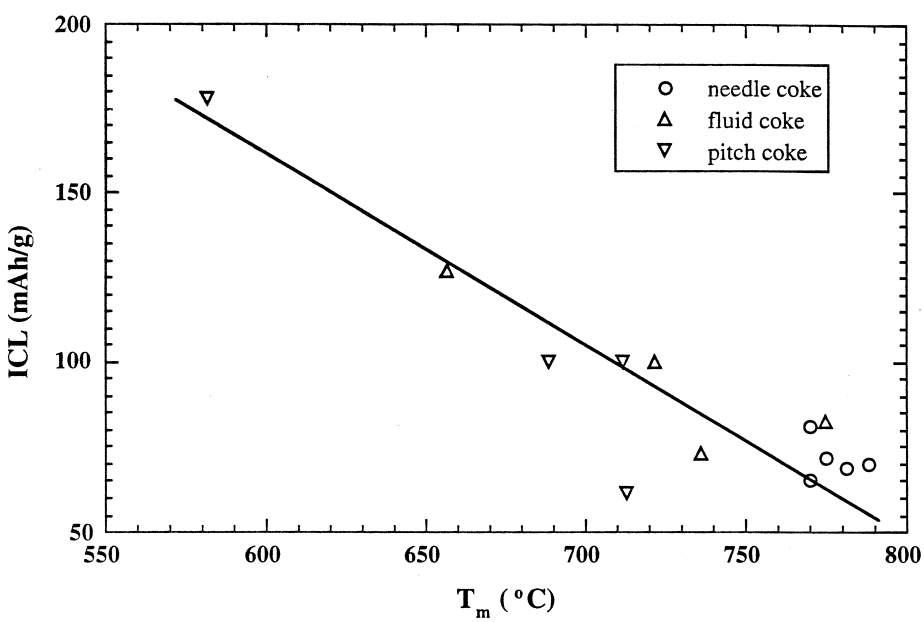

Fig. 3. Plot of T_m vs. ICL for petroleum (fluid and needle coke) and coal-tar pitch cokes in 0.5 M $LiN(CF_3SO_2)_2$ in 50:50 EC-DMC. Line indicates trend of the data.

concentration of active sites decreases with an increase in L_a. If L_a is associated with the active sites, and if ICL is a function of the active surface area, then it should be possible to draw a correlation between L_a and ICL. The following analysis presents a simple model for such a correlation.

In this analysis electrolyte decomposition associated with the ICL is assumed to occur on the active sites on carbon, which are considered to be edge sites. It is further assumed that the amount of active edge sites is a function of the crystallite parameters, L_c and L_a. Recently, Chung et al. [7] determined the ICL on a variety of carbons (e.g., natural and artificial graphite, mesocarbon microbeads, and carbon fibers), and they concluded that the rate of electrolyte decomposition on the basal plane was about 1/6 that on the edge sites. The conclusions by Winter et al. [5] and Chung et al. [7] are consistent with the assumption that the edge plane sites are the dominant active sites for electrolyte decomposition.

A schematic representation for a simple prismatic structure of a carbon crystallite that consists of basal and edge sites, and the corresponding crystallite parameters, L_a and L_c, are presented in Fig. 4. A structure in which the dimensions of the basal plane is given by $L_a \times L_a$ vastly simplifies the analysis. A carbon particle is assumed to be a collection of crystallites, which is illustrated by the array $(a \times b \times c)$ shown in Fig. 4. In the schematic representation presented in Fig. 4, $a = 6$, and $b = c = 2$. A larger

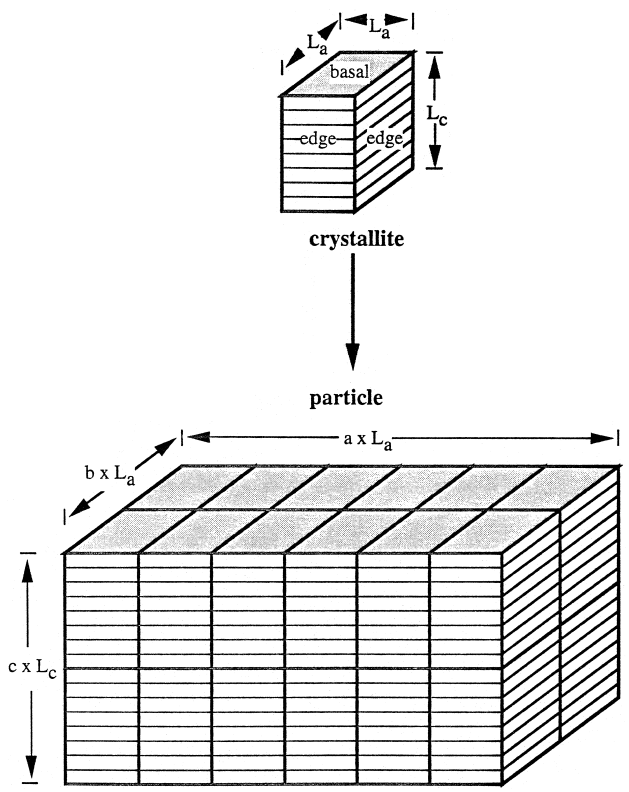

Fig. 4. Schematic representation of a model for carbon crystallite and particle.

particle is obtained by simply adding more crystallites to the structure (increasing a, b and c), and the shape of the particle is determined by the arrangement of the crystallites (vary the relative values of a, b and c). The depiction by Spain [35] of a particle of turbostratic graphite suggests that the graphite crystallites are stacked in some regular arrangement but the individual crystallite may be tilted with respect to each other. Because the stacking arrangement allows for voids between the crystallites, the density is lower than that corresponding to perfect graphite. The arrangement of crystallites illustrated in Fig. 4 assumes that there are no pores present in the particle. This is a gross simplification because the typical carbon particle has a density less than the theoretical value (2.25 g/cm^3), which suggests that some open and/or closed pores are present. The open pores will contribute to a higher surface area than that expected for a solid carbon particle of theoretical density. Furthermore, defects that expose additional surface sites are not considered in the model.

As a practical illustration of the crystallite dimension, the L_c of some natural graphites are large, i.e., about 1 mm [35]. Artificial graphites such as highly oriented pyrolytic graphite (HOPG) are also produced with L_c of 0.1 μm and L_a of ≥ 1 μm, and L_a may be as large as 4–10 μm [35]. The graphitizable carbons and graphite powders used in the present study have much smaller crystallite dimensions than that of HOPG.

The volume (V_c) of the crystallite depicted in Fig. 4 is given by

$$V_c = L_a^2 L_c \tag{4}$$

Fujimoto et al. [36,37] examined the crystallite dimension of prismatic graphite and obtained

$$V_c = \left(3\sqrt{3}/8\right) L_a^2 L_c \tag{5}$$

for the volume of a hexagonal crystallite, which is not too different from the expression in Eq. (4). The volume of the particle in Fig. 4 is the sum of the total number of crystallites,

$$V = abc\, L_a^2 L_c \tag{6}$$

The mass of the particle (M) is simply

$$M = V\rho = abc\, L_a^2 L_c\, \rho \tag{7}$$

where ρ is the density of the carbon. This model is more appropriate for soft carbons (i.e., graphitic carbons) which have low porosity, but is not a good representation for hard carbons that usually have high porosity. The active surface area (s_{act}) is equal to the total area of the edge sites (s_e) that is present, or

$$s_{act} = s_e = 2c\, L_a L_c (a + b) \tag{8}$$

The specific active surface area, S_{act} (area/weight), is given by

$$S_{act} = s_{act}/M = 2c\, L_a L_c (a + b)/\left(abc\, L_a^2 L_c\, \rho\right) = 2(a + b)/(ab L_a \rho) \tag{9}$$

From this relationship, it is apparent that the specific active surface area increases as the crystallite dimension L_a decreases, assuming that the number of crystallites and density are constant. Closer examination of the effect of the crystallite parameters in Fig. 4 on the active surface area leads to the same conclusion. Take for example the situation where $L_a \ll L_c$. In this case the area of the basal plane $(L_a \times L_a)$ is much smaller than that of the active sites $(L_a \times L_c)$, and the net result is a higher relative fraction of active surface area. Alternatively, when $L_a \gg L_c$, the fraction of active surface area of the crystallite is lower. This simple analogy illustrates the significant role of L_c and L_a on the active surface area of carbon crystallites.

Assuming that ICL is proportional to the active surface area, we can derive the following relationship

$$\mathrm{ICL(mA\,h/g)} \propto s_{\mathrm{act}}/V\rho \propto 2cL_aL_c(a+b)/(abcL_a^2L_c\rho) \quad (10)$$

and

$$\mathrm{ICL(mA\,h/g)} = K'(a+b)/(abL_a) = K/L_a \quad (11)$$

where K is proportionality constant that is a function of the reactivity of the edge sites and the number of crystallites in the particle. The morphology of needle cokes is approximated by a particle shape where $aL_a \gg bL_a$, $aL_a \gg cL_c$, and correspondingly, the fluid and pitch cokes may have a morphology that is closer to an arrangement of crystallites where $aL_a \equiv bL_a \equiv cL_c$. In either case, Eq. (10) simplifies to a relationship where ICL is inversely proportional to L_a. This analysis predicts that ICL is a function of the active surface area, and a linear relationship should be obtained when ICL is plotted as a function of $1/L_a$.

3.3. Data analysis

The experimental studies presented in Figs. 1 and 2 were conducted with a variety of electrodes and electrolytes, consequently it complicates rationalizing these results. If the specific ICL activity of a carbon is uniform over its surface, then a horizontal curve should be obtained as a function of surface area in Fig. 1. Because of the varying specific activity that is observed, it is apparent that different surface sites are present where the activity is not the same. However, the physical meaning of the trend in terms of the structural properties of carbon and the role of different electrolytes in the observed results is still not clearly understood.

The validity of Eq. (11) was examined by analyzing experimental results for ICL and physical properties (i.e., crystallographic parameters, BET surface area) of various carbons. The types of carbons, electrolytes and references to the experimental data are listed in Table 1. Both hard and soft carbons are included in the study, as well as different electrolytes.

The data compiled for ICL is plotted as a function of $1/L_a$ in Fig. 5. The scatter in the plot is large, which we attribute to the use of data for both hard and soft carbons, as well as the different conditions used to obtained the ICL results. Despite this scatter, we believe that the trend shows that ICL is inversely proportional to L_a. This relationship is consistent with the predicted result from Eq. (11). As discussed above, the proportionality constant K is expected to vary with the different types of carbons used in the analysis because the density of the different carbons is not the same and the regular particle geometry shown in Fig. 4 is unlikely to exist. For example, the density in-

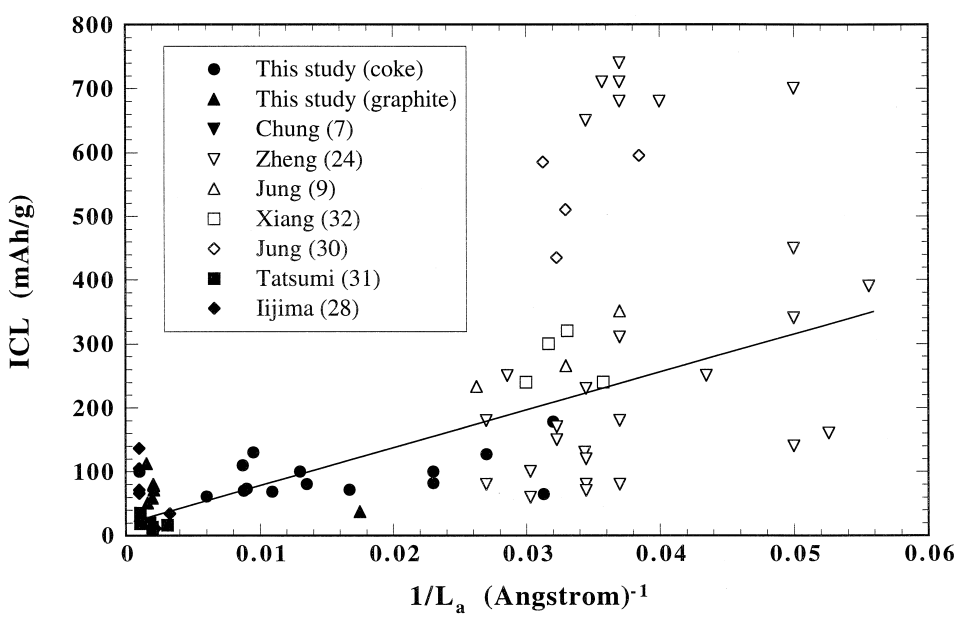

Fig. 5. Composite plot of ICL vs. $1/L_a$. See Table 1 for source of the data. Line indicates trend of the data.

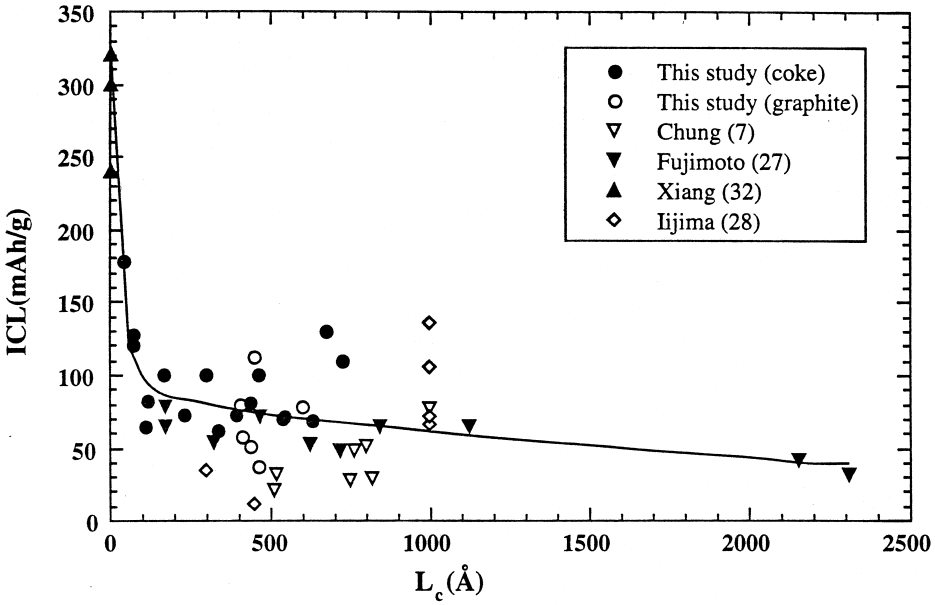

Fig. 6. Composite plot of ICL vs. L_c. See Table 1 for source of the data. Line indicates trend of the data.

creases with the increasing heat-treatment temperature of graphitizable carbons [30], and the parameters *a*, *b* and *c* change with particle size and morphology. Therefore, it is not too surprising to observe large scatter in the plot in Fig. 5. Despite these shortcomings, the trend observed in Fig. 5 suggests agreement with the prediction of Eq. (11).

The crystallite parameters, L_a and L_c, and the $d(002)$ spacing change with heat treatment of graphitizable carbons. The crystallite parameters increase, and the $d(002)$ spacing decreases, with increasing heat-treatment temperature. As noted in Part 1 [21], the change of these parameters with heat treatment will vary with the carbon precursor. The increase in L_c and decrease in $d(002)$ spacing will also reduce the relative amount of active sites present in the graphitizable carbon and this should be reflected in the relationship with ICL. Figs. 6 and 7 show plots of ICL vs. L_c and $d(002)$ spacing, respectively. The trend of ICL is consistent with the prediction that the amount of active

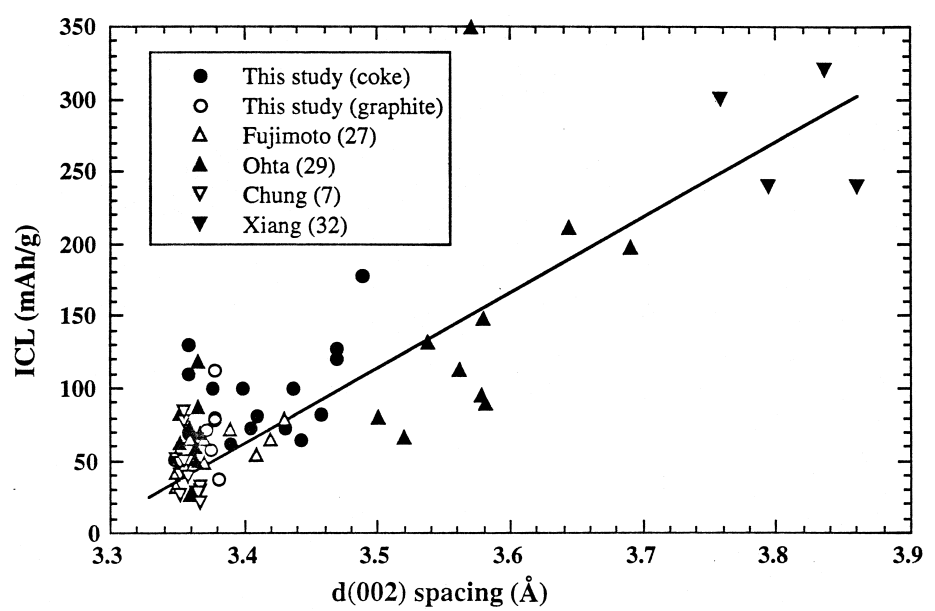

Fig. 7. Composite plot of ICL vs. $d(002)$ spacing. See Table 1 for source of the data. Line indicates trend of the data.

sites decreases with an increase in L_c and a decrease in $d(002)$ spacing. The ICL decreases with an increase in L_c and a decrease in $d(002)$ spacing.

Interpreting the relationship between the ICL of carbons for Li storage and the physical structure of carbons is not straightforward for several reasons. First, the crystallographic parameters, $d(002)$ spacing, L_a and L_c, are highly variable. These parameters vary with the surface area, particle size and processing conditions of the carbon. Second, these parameters cannot be independently varied. Heat treatment of carbon will affect each of these parameters in a predictable but mainly uncontrolled manner that also depends on the carbon precursor. For example, heat treatment of soft carbons at high temperatures (>2000°C) will decrease the $d(002)$ spacing and increase L_a and L_c. On the other hand, hard carbons do not necessarily show the same trends upon heat treatment. The BET surface area is one parameter that has been correlated to the electrochemical performance of carbons for Li-ion batteries. Matsumura et al. [38] reported that the reversible capacity of disordered carbon increases linearly with the parameter $[1/(L_c/d(002)+1)]$, which they consider to be proportional to the surface area of the crystallite. Unfortunately their studies indicated that this relationship was not valid for graphitic materials (i.e., $L_c > 100$ Å). In the present paper, we have extended the earlier analysis by considering the significance of the crystallographic parameters, L_a and L_c, of carbon on the ICL. The analysis concludes that L_a and L_c are parameters that relate to the active surface area of carbon, and it is this surface area and not the total surface area that determines the ICL of carbons in Li-ion batteries.

4. Concluding remarks

The importance of carbon active sites on the ICL is deduced from an analysis of crystallographic parameters. The results obtained by thermal analysis and measurements of crystallographic parameters, L_a and L_c, and the $d(002)$ spacing, are used to illustrate the relationship between the ICL and the active sites on carbon. Based on an analysis of the results from this study and published data, we conclude that the active surface area and not the total BET surface area is the important factor contributing to the magnitude of the ICL on carbons for Li-ion batteries. This conclusion suggests that the carbon surface structure is an important factor in catalyzing electrolyte decomposition.

Acknowledgements

This work was supported by the Assistant Secretary for Energy Efficiency and Renewable Energy, Office of Advanced Automotive Technologies of the U.S. Department of Energy under Contract No. DE-AC03-76SF00098 at Lawrence Berkeley National Laboratory, Contract No. W-7405-ENG-48 at Lawrence Livermore National Laboratory and Contract No. 6455828 at the University of Michigan. The authors would like to acknowledge Superior Graphite for kindly supplying the carbon samples used in this study. We would also like to acknowledge Mr. W. Jiang for the thermal analysis measurements; and Dr. G. Chung for providing an advance copy of his manuscript on ICL on carbon and for fruitful discussion on the relationship between ICL and the structure of carbon.

References

[1] R. Fong, U. von Sacken, J. Dahn, J. Electrochem. Soc. 137 (1990) 2009.
[2] F. Disma, L. Aymard, L. Dupont, J. Tarascon, J. Electrochem. Soc. 143 (1996) 3959.
[3] K. Takei, N. Terada, K. Kumai, T. Iwahori, T. Uwai, T. Miura, J. Power Sources 55 (1995) 191.
[4] M. Terasaki, H. Yoshida, T. Fukunaga, H. Tukamoto, M. Mizutani, M. Yamachi, GS News Tech. Rep. 53 (1994) 23.
[5] M. Winter, P. Novak, A. Monnier, J. Electrochem. Soc. 145 (1998) 428.
[6] E. Barsoukov, J. Kim, C. Yoon, H. Lee, J. Electrochem. Soc. 145 (1998) 2717.
[7] G.-C. Chung, S.-H. Jun, K.-Y. Lee, M.-H. Kim, J. Electrochem. Soc. 146 (1999) 1664.
[8] E. Peled, D. Bar-Tow, A. Melman, E. Gerenrot, Y. Lavi, Y. Rosenberg, in: N. Doddapaneni, A. Landgrebe (Eds.), Proceedings of the Symposium on Lithium Batteries, Vol. 94-4, The Electrochemical Society, Pennington, NJ, 1994, p. 177.
[9] Y. Jung, M. Suh, S. Shim, J. Kwak, J. Electrochem. Soc. 145 (1998) 3123.
[10] T. Tran, K. Kinoshita, J. Electroanal. Chem. 386 (1995) 221.
[11] O. Yamamoto, Y. Takeda, R. Kanno, in: B. Barnett, E. Dowgiallo, G. Halpert, Y. Matsuda, Z. Takehara (Eds.), Proceedings of the Symposium on New Sealed Rechargeable Batteries and Supercapacitors, Vol. 93-23, The Electrochemical Society, Pennington, NJ, 1993, p. 302.
[12] D. Bar-Tow, E. Peled, L. Burstein, in: C. Holmes, A. Landgrebe (Eds.), Proceedings of the Symposium on Batteries for Portable Applications and Electric Vehicles, Vol. 97-18, The Electrochemical Society, Pennington, NJ, 1997, p. 324.
[13] J. Besenhard, H. Fritz, J. Electroanal. Chem. 53 (1974) 329.
[14] M. Armand, P. Touzain, Mat. Sci. Eng. 31 (1977) 319.
[15] H. Shiota, H. Kimura, H. Urushibata, in: Proceedings of International Workshop on Advanced Batteries (Lithium Batteries), Osaka, Japan, February 22–24, 1995, p. 311.
[16] E. Charsley, J. Dunn, Rubber Chem. Technol. 55 (1982) 382.
[17] A. Kirshenbaum, Thermochim. Acta 18 (1977) 113.
[18] T. Honda, T. Saito, Y. Horiguchi, Tanso 72 (1972) 14.
[19] N. Welham, J. Williams, Carbon 36 (1998) 1309.
[20] L. Radovic, P. Walker, R. Jenkins, Fuel 62 (1983) 849.
[21] W. Jiang, T. Tran, X. Song, K. Kinoshita, Part 1, submitted J. Power Sources.
[22] T. Tran, L. Spellman, W. Goldberger, X. Song, K. Kinoshita, J. Power Sources 68 (1997) 106.
[23] T. Tran, J. Feikert, X. Song, K. Kinoshita, J. Electrochem. Soc. 142 (1995) 3297.
[24] T. Zheng, Y. Liu, E. Fuller, S. Tseng, U. von Sacken, J. Dahn, J. Electrochem. Soc. 142 (1995) 2581.
[25] E. Buiel, A. George, J. Dahn, J. Electrochem. Soc. 145 (1998) 2252.
[26] E. Buiel, J. Dahn, J. Electrochem. Soc. 145 (1998) 1977.

[27] M. Fujimoto, K. Ueno, T. Nohma, M. Takahashi, K. Nishio, T. Saito, in: B. Barnett, E. Dowgiallo, G. Halpert, Y. Matsuda, Z. Takehara (Eds.), Proceedings of the Symposium on New Sealed Rechargeable Batteries and Supercapacitors, Vol. 93-23, The Electrochemical Society, Pennington, NJ, 1993, p. 281.
[28] T. Iijima, K. Suzuki, Y. Matsuda, Synth. Met. 73 (1995) 9.
[29] A. Ohta, H. Koshina, H. Okuno, H. Murai, J. Power Sources 54 (1995) 6.
[30] Y. Jung, M. Suh, H. Lee, M. Kim, S. Lee, S. Shim, J. Kwak, J. Electrochem. Soc. 144 (1997) 4279.
[31] K. Tatsumi, K. Zaghib, Y. Sawada, H. Abe, T. Ohsaki, J. Electrochem. Soc. 142 (1995) 1090.
[32] H. Xiang, S. Fang, Y. Jiang, J. Electrochem. Soc. 144 (1997) L187.
[33] Y. Matsumura, S. Wang, J. Mondori, J. Electrochem. Soc. 142 (1995) 2914.
[34] E. Peled, C. Menachem, D. Bar Tow, A. Melman, J. Electrochem. Soc. 143 (1996) L4.
[35] I. Spain, Chemistry and Physics of Carbon 16 (1981) 119.
[36] H. Fujimoto, K. Tokumitsu, A. Mabuchi, T. Kasuh, M. Shiraishi, Carbon 32 (1994) 193.
[37] H. Fujimoto, K. Tokumitsu, A. Mabuchi, T. Kasuh, M. Shiraishi, Carbon 32 (1994) 1249.
[38] Y. Matsumura, S. Wang, J. Mondori, Carbon 33 (1995) 1457.